Prepared for ARS/ANS/IAS
Nuclear Propulsion Conference
Aug. 15-17, 1962
Monterey, Calif.

E-1684

# ON THE HYDRODYNAMICS OF A COAXIAL FLOW GASEOUS REACTOR

By Robert G. Ragsdale and Herbert Weinstein

Lewis Research Center
National Aeronautics and Space Administration
Cleveland, Ohio

## Introduction

The concept of a coaxial flow gaseous reactor is presented in reference 1, and will be but briefly described here. The containment criterion, common to all gaseous reactor schemes, is met by introducing a slow moving stream of fissionable gas into a surrounding, fast moving stream of hydrogen propellant. The hydrodynamic analysis of such a system must include both mass and momentum interchange between the two streams, and is additionally complicated by heat transfer and criticality considerations. The approach here has been to first restrict attention to an isothermal, laminar coaxial flow system.[2] This basic analysis has been extended in this paper to include turbulence by introducing an eddy diffusivity into the laminar equations.

Experimental measurements have been made on an air-bromine coaxial flow system. Measured values of the variation of inner stream (bromine) density with axial position are compared with the analysis for both laminar and turbulent flow of the outer (air) stream. The purpose of this study is to verify the fundamental diffusion and momentum transfer analysis. Though the additional complexities associated with flow instability and nuclear heat generation are as yet unexplored, the results presented here provide necessary information about the basic mixing process in a coaxial flow gaseous reactor.

## Analysis

The assumptions and restrictions made in deriving the equation set for the model shown in figure 1 are: (1) the entire flow field is at steady state and constant temperature and pressure, (2) axial symmetry exists, (3) the fluids mix ideally, and (4) the usual boundary layer assumptions apply.

The equation set consists of the continuity equation with the steady state and axial symmetry assumptions; the momentum equation, which is the axial component Navier-Stokes equation, with the boundary layer, steady state, axial symmetry, constant pressure and constant temperature assumptions; and the diffusion equation[3] with the axial symmetry and steady state assumptions. These three equations are taken through a transformation to an axial length-stream function coordinate set.

The resulting equations are:

momentum: $$\frac{\partial \bar{u}}{\partial \bar{z}} = \frac{\beta + 1}{Re_{1,0}} \cdot \frac{\partial}{\partial \psi}\left[\bar{\mu}\bar{r}^2 \bar{u}(\beta C + 1)\frac{\partial \bar{u}}{\partial \psi}\right] \qquad (1)$$

diffusion: $$\frac{\partial C}{\partial \bar{z}} = \frac{(\beta C + 1)^2}{Re_{1,0} \cdot Sc_{1,0}} \cdot \frac{\partial}{\partial \psi}\left[\bar{D}\bar{r}^2 \bar{u}\frac{\partial C}{\partial \psi}\right] \qquad (2)$$

where

$\bar{u} = \dfrac{\text{Local axial velocity}}{\text{Initial inner stream velocity}}$; $\psi$ = stream function

$\bar{z} = \dfrac{\text{Axial distance}}{\text{Initial inner stream radius}}$; $\bar{\mu} = \dfrac{\text{Local mixture viscosity}}{\text{Inner stream viscosity}}$

$\beta = \dfrac{\text{Mol. wt. of inner stream}}{\text{Mol. wt. of outer stream}} - 1$; $C$ = Inner stream mole fraction

$\bar{r} = \dfrac{\text{Radial distance}}{\text{Initial inner stream radius}}$; $\bar{D} = \dfrac{\text{Local binary diff. coeff.}}{\text{Inner stream self-diff. coeff.}}$

$Sc_{1,0}$ = Initial inner stream Schmidt number; $Re_{1,0}$ = Initial inner stream Reynolds number

Because of the cylindrical geometry, the radial distance does not drop out of the equations as it would in a two-dimensional system as Pai[4] showed, so a form of the continuity equation must be carried along in the numerical integration to relate $\bar{r}$ and $\psi$. The form used is obtained by assuming again $\partial\psi/\partial\bar{r} \gg \partial\psi/\partial\bar{z}$ and dropping the term containing the smaller derivative:

continuity: $$\int_0^{r} \bar{r}'\,d\bar{r}' = \int_0^{\psi} \frac{1}{\bar{u}(\beta C + 1)}\,d\psi' \qquad (3)$$

These equations are integrated numerically from the initial face at the nozzle entrance downstream to a face beyond the end of the potential core.

The laminar analysis is extended to include turbulent flow by introducing eddy diffusivity factors into the molecular viscosity and diffusivity terms in the above equations. This is done in the usual manner:

$$\mu_{turb} = \mu_{lam}\,(1 + \rho\epsilon/\mu_{lam})$$

$$D_{turb} = D_{lam}\,(1 + \epsilon/D_{lam})$$

for both fluids. In addition, the value of $(\rho\epsilon/\mu)$ in the inner stream is allowed to vary axially from a low initial value up to the constant value of the $(\rho\epsilon/\mu)$ in the outer stream according to the form:

$$(\rho\epsilon/\mu)_1 = (\rho\epsilon/\mu)_{1,0} + a_1(\bar{z})^{a_2}.$$

Experiment

The air-bromine coaxial flow test set-up is shown schematically in figure 2. Metered air is introduced through a tube bundle, and flows downward in a five inch by five inch Lucite channel. A metered bromine stream is injected into the air stream two feet downstream from the tube bundle through a one-half inch diameter monel tube. The test section was operated at five psia, the vapor pressure of bromine at room temperature. A photograph of the test apparatus is shown in figure 3.

Radial average bromine concentrations were measured at one-inch intervals downstream from the point of injection by a light absorption technique. One-eighth inch diameter collimated light beams were passed through the bromine stream, and intercepted by photomultiplier detectors. Concentration was calculated from the measured light attenuation from Beer's law.

The calculated concentrations at the various axial stations were normalized to the value at the injection point, and are thus independent of the absolute value of absorption coefficient. This concentration ratio, $\underline{C}^*$, is plotted as a function of the distance from the injection point, $\bar{z}$, normalized to the initial bromine stream radius. Two flow conditions are reported here; one is for laminar flow of both streams, and the other for turbulent.

Discussion of Results

Figure 4(a) shows a comparison of the experimental data with the analysis for laminar flow. The Reynolds number of the airstream is 2075, and the initial air-to-bromine velocity ratio is 4.3. The initial bromine Reynolds number, based on the diameter of the injection tube, is 200. The agreement is satisfactory in view of the relatively complex flow mechanism under consideration. Two factors are worthy of note here. First, though the Reynolds numbers of both the air and bromine streams are within the laminar regime, the discontinuity resulting from the finite thickness of the injection tube tended to introduce a certain amount of turbulence. Second, the analytical line is a true radial average, while the experimental conditions only approximate this, since the light beams were of finite diameter. Both of these considerations would tend to cause the data to fall somewhat below the predicted line.

For laminar flow, the conditions of the experiment are used as input to the analysis, and the predicted variation of concentration with axial position is obtained. For turbulent flow, the situation is not so well defined. In addition to the measurable parameters, one more quantity is required but unavailable. That is the value of a turbulence level factor, $(\rho\epsilon/\mu)$. In the outer stream, this factor is considered constant. In the bromine stream, the turbulence factor is allowed to vary from some initial value (zero, if the bromine stream is initially laminar) up to the $(\rho\epsilon/\mu)$ in the airstream.

It is possible, however, to estimate this parameter from the Reynolds number, based on existing pipe flow data. This was done, and for the turbulent case considered here, the $(\rho\epsilon/\mu)$ of the airstream was estimated to be from 10 to 20. For this run, the air Reynolds number was 10,000, and the initial bromine Reynolds number was 3020. The initial air-to-bromine velocity ratio was 1.4.

Figure 4(b) shows the experimental data for these conditions. The predicted line for laminar flow is shown for comparison. The analytical line for turbulent flow was obtained by taking a turbulence factor of 12 for both the air and bromine streams. Since this value is within the range expected from pipe flow information, the procedure seems justified; though, admittedly, this probably masks certain experimental inaccuracies. A more realistic approach would be to consider some initially low turbulence level factor in the bromine stream, and allow it to increase axially to the airstream value. The point of view here is that, for the purposes of this paper, it is sufficient to show that the assumption of equal turbulence levels in the two streams yields satisfactory results.

Additional data, over a range of flow conditions, would be required to determine a relationship between turbulence level and Reynolds number for a coaxial flow system. The three flow regimes of interest are: (1) laminar flow of both streams, (2) turbulent flow of both streams, and (3) laminar flow of the inner stream and turbulent flow of the outer stream. The general agreement of the experimental data and the analysis for both turbulent flow (with an assumed value of $\rho\epsilon/\mu$) and laminar flow cases presented here indicates that the important physical mechanisms for mass and momentum transfer are adequately described by the analytical expressions.

REFERENCES

1. Weinstein, Herbert, and Ragsdale, Robert G.: A Coaxial Flow Reactor - A Gaseous Nuclear-Rocket Concept. ARS preprint 1518-60, Dec. 5, 1960.

2. Weinstein, Herbert, and Todd, Carroll A.: A Numerical Solution of the Problem of Mixing of Laminar Coaxial Streams of Greatly Different Densities - Isothermal Case. NASA TN (to be published).

3. Bird, R. B., Stewart, W. E., and Lightfoot, E. C.: Notes on Transport Phenomena. Wiley & Sons, New York, 1958.

4. Pai, Shih-I: Fluid Dynamics of Jets. Van Nostrand Co., New York, 1958.

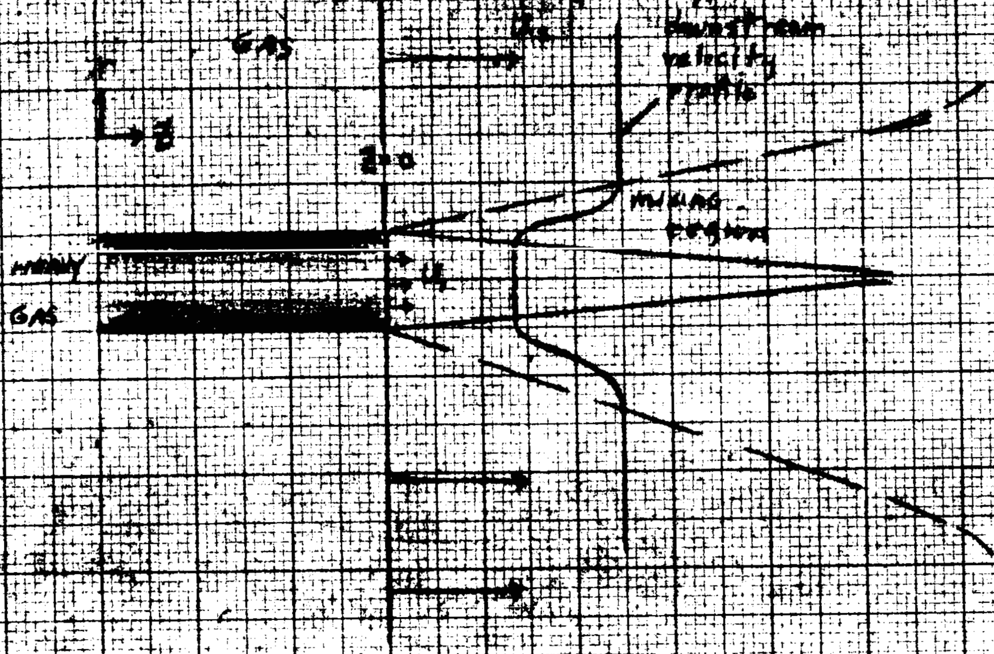


FIG 1 - COAXIAL FLOW MODEL

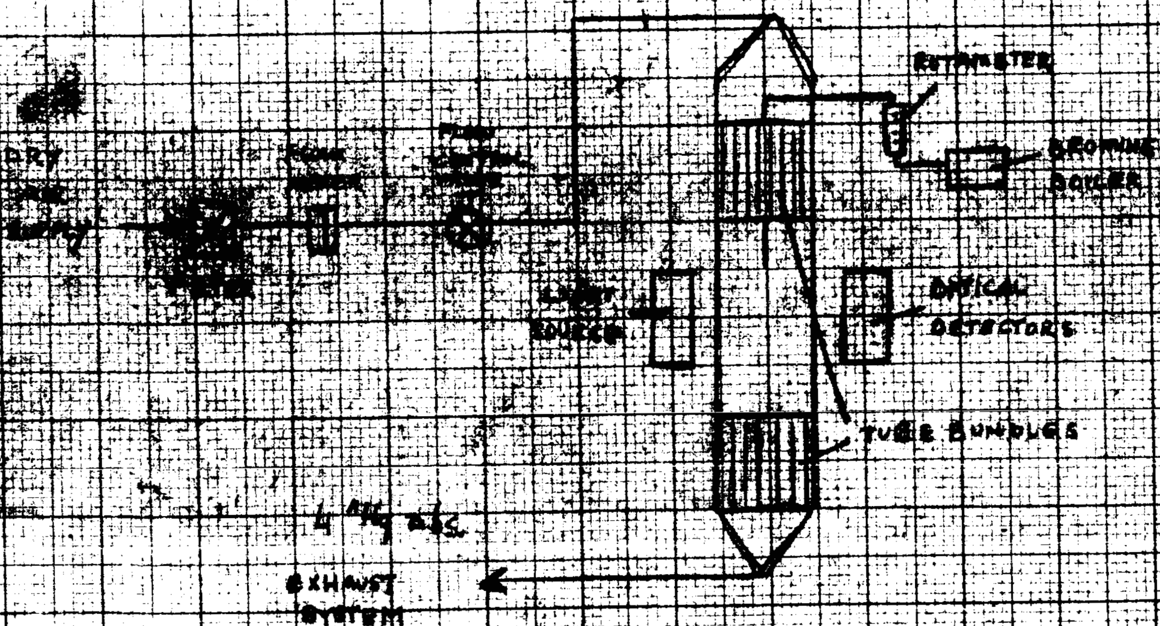


FIG 2 - SCHEMATIC OF AIR-BROMINE SYSTEM

ASA
C-55685

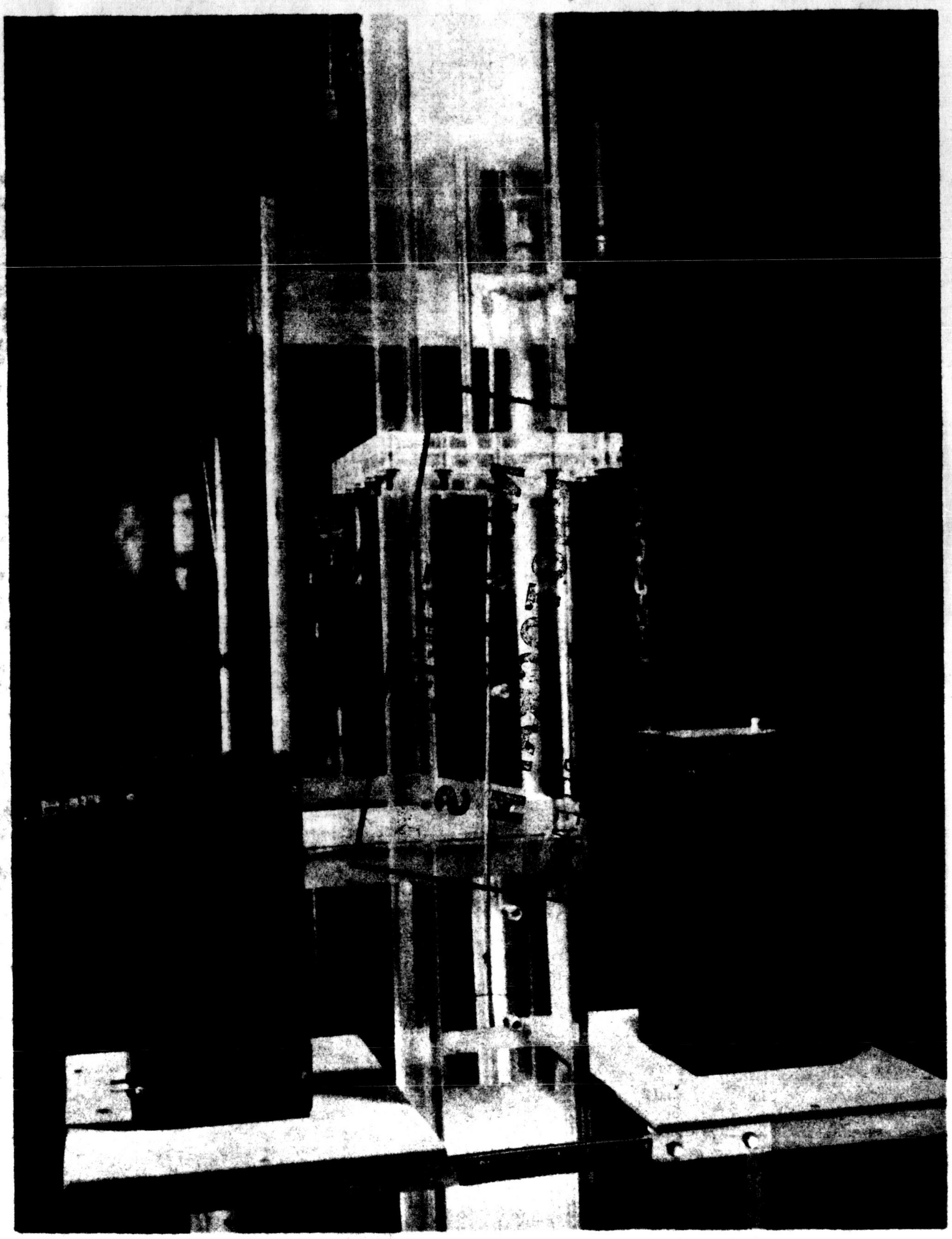

Figure 3. - Air-bromine test apparatus.

FIGURE 4 - AIR-BROMINE COAXIAL FLOW TESTS

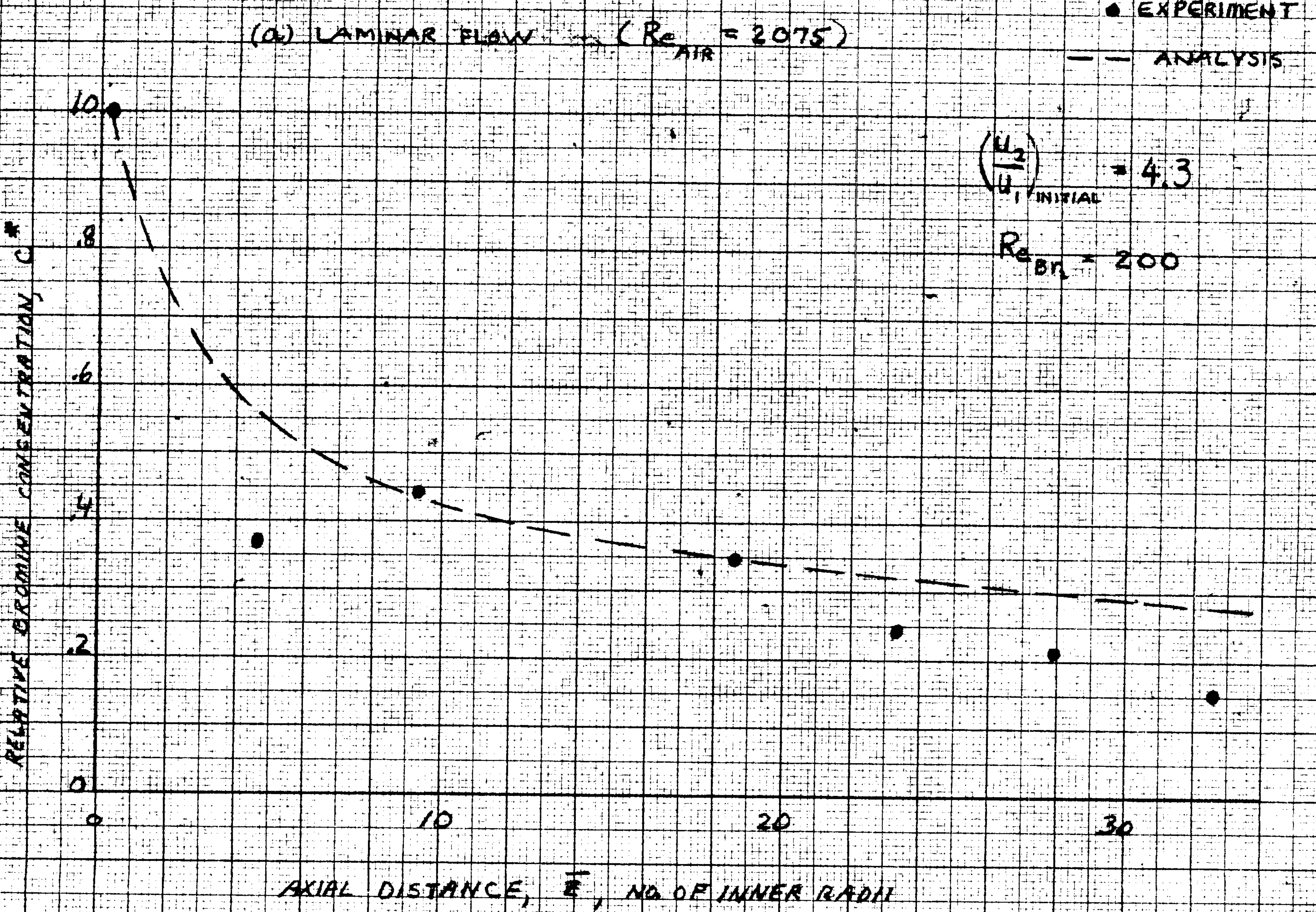

# FIGURE 4 - AIR-BROMINE COAXIAL FLOW TESTS